Template Effects in Porous Coordination Polymers[†]

Daisuke Tanaka and Susumu Kitagawa*

Department of Synthetic Chemistry and Biological Chemistry, Kyoto University, Katsura, Nishikyo-ku, Kyoto 615-8510, Japan

Received November 8, 2007

In recent years, a new class of porous materials based on a combination of organic components and metal centers has emerged, called porous coordination polymers (PCPs). PCPs have unique characteristics: regular nanosized spaces, flexibility, and a designed pore surface. The interaction between PCP nanospaces and guest molecules controls the nanoscale molecular assembly. In this short review, correlations between PCPs and guest molecules will be introduced under the rubric of "template".

1. Introduction

In recent years, many porous coordination polymers (PCPs) or metal−organic frameworks have been synthesized, providing a variety of properties such as storage, exchange, catalysis, and magnetic and optical properties.[1–7] The nanospaces of PCPs have unique characteristics: regular nanosized pores, flexibility, and a designed pore surface that can create unprecedented porous functionalities. In particular, the pore properties are prerequisites for the efficient accommodation of specific guest molecules. The well-designed inclusion of a target molecule is responsible for high selectivity and/or an ordered array of guest molecules, which are regarded as a new class of materials. On the other hand, the structures and properties of PCPs can be controlled by some molecules or ions occluded in their pores. The interplay between guest and host entity can provide strategies for the design and synthesis of functional porous materials.

Generally, the pores of PCPs are initially filled with the solvent used in the synthesis reaction, such as water, which acts as a template. The structure and chemical properties of guest template molecules can be transcribed into pore shapes and properties. In addition, PCPs have flexible and dynamic natures.[8–10] Flexible frameworks give rise to structural rearrangements, i.e., the transformation from a "closed" phase to an "open" phase for guest molecules. The inclusion of template species in flexible PCPs is associated with switching of structures and/or properties. In this sense, guest molecules, or templates, could be keys for dynamic frameworks for PCPs, which are dissimilar to the template synthesis of MCM-41.[11]

On the other hand, the confinement effects of pores can be considered as a stabilization effect that enables the preparation of an ordered array or condensed phase of specific molecules that is not stable as a bulk fluid.[12,13] The well-regulated and designable pores of PCPs could shape the specific molecular arrays characteristic of nanospaces. Unique molecular assemblies in a nanometer-sized space would lead not only to finding novel phenomena but also to providing novel magnetic, electric, and photophysical properties. The pores of PCPs can thus work as templates, and their confinement effect can control the orientation and/or conformational arrangement of the guest molecules.

We survey the interactions and correlations between PCPs and guest molecules under the rubric of "template". Focused

Scheme 1. Template Effects in PCPs

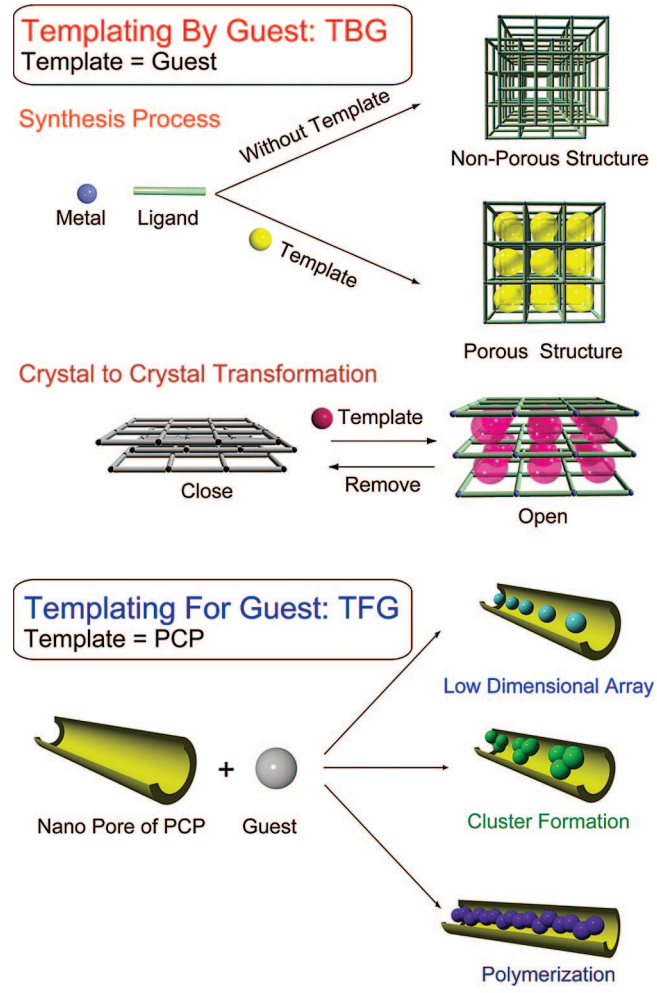

[†] Part of the "Templated Materials Special Issue".

* Corresponding author. E-mail: kitagawa@sbchem.kyoto-u.ac.jp.

10.1021/cm7031866 CCC: $40.75
Published on Web 12/15/2007

on the relationship between the pores and guest molecules, the template effect in PCPs can be divided into two types (Scheme 1):

(a) Templating by guests, TBG: guest molecules act as a template. A template species is an isolated small molecule and is included as an isolated entity in the PCP framework.

(b) Templating for guests, TFG: PCP frameworks act as a template. The PCP framework provides a scaffold with voids.

This classification is an analogy to that made in inorganic mesoporous materials.[14]

We use the two concepts to describe a logical approach to the design and synthesis of functional materials.

2. TBG: Guest Molecules Acting as Templates

TBG creates not only voids but also coordination frameworks, which is similar to mesoporous material synthesis.[14] With PCPs, however, only one or several isolated small molecules act as templates; therefore, the shape and functional groups of the template molecule play a crucial role. The TBG in the synthesis processes is called "primary TBG". In addition, PCPs are often much more dynamic than generally believed. When such flexible PCPs accommodate template molecules, guest information strongly affects host structures, which is a new type of TBG effect. This dynamic template effect is defined as "secondary TBG". In the following context, we will introduce the two types of TBG effects in PCPs.

2.1. Primary TBG: Template Effects in the PCP Synthesis Process. Coordination polymers contain two central components: connectors (metal ions) and linkers (bridging ligands). These are defined as the starting reagents with which the principal framework of the coordination polymer is constructed. A huge number of structural topologies of the frameworks of coordination polymers and inorganic materials have been reported, and excellent reviews have been published.[15–18] In the design and synthesis of "porous" architectures using these frameworks, the key factor is to preclude dense structures and to control the shapes and sizes of the pores. In other words, the control of "supramolecular isomerism", the existence of more than one superstructure for a given set of components, is of particular importance.[16,19] Generally, it is impossible to synthesize compounds containing vacant spaces, as nature abhors a vacuum. Hence, the pores will always initially be filled with guest molecules. One of the available tactics for constructing a desired open framework is using appropriate guest or template molecules, because self-inclusion is prevented by exploiting noncovalently bound organic guests as placeholders in the overall lattice, resulting in guest-templated pores. This template effect is called "primary TBG".

Coordination polymers with square-planar or octahedral metal ions and linear bifunctional "spacer" or "rod" ligands such as 4,4′-bipyridine (bipy) tend to give square-grid sheets. Among these compounds, mutual interpenetration of the sheets often occurs, and, therefore, no porous frameworks are formed (Scheme 2).[20] However, 2D grid structures of nickel(II)- and bipy-containing pyrene as guest molecules,

Scheme 2. Endotemplating Effect in Square-Grid Architecture Synthesis

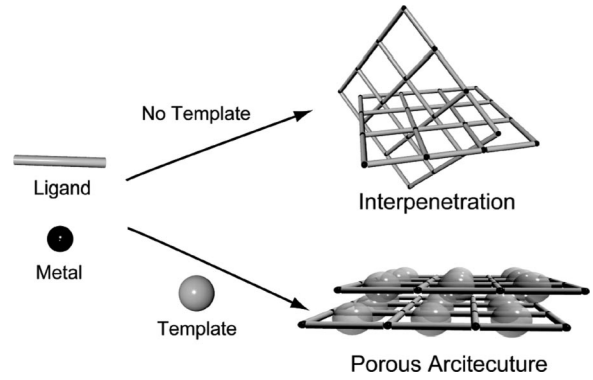

$\{[Ni(4,4'\text{-bipy})_2(NO_3)_2]\cdot 2\text{pyrene}\}_n$, provide open-coordination frameworks.[21] In the structure, the pyrene molecules form a noncovalent (4,4) network that is complementary from a topological perspective to the square-grid coordination polymer network. The structure can be described as the interpenetration of a noncovalent net and a square-grid coordination polymer. The interpenetration of host frameworks and guest nets prevents the mutual interpenetration of host frameworks. A longer ligand, 9,10-bis(4-pyridyl)anthracene (bpa), and $Ni(NO_3)_2$ form a mutually interpenetrating 2D grid structure $\{[Ni(bpa)_2(H_2O)_2]\cdot 2NO_3\}_n$ in the presence of benzene.[22] On the other hand, bpa forms open-square-grid coordination polymers with $Ni(NO_3)_2$ or $Cu(NO_3)_2$ only in the presence of electron-deficient guest molecules such as nitrobenzene or cyanobenzene because of the donor–acceptor interactions between the anthracene moiety and the guest molecules. The use of electron-deficient (or electron-rich) template molecules paved the way for open network structures of electron-rich (or electron-deficient) ligands.

In the presence of appropriate molecular templates, different-sized pores can be isolated. For instance, simple imidazolate derivatives are bent exobidentate ligands and can be expected to show a linear or slightly bent im−Cu^I−im geometry in binary copper(I) imidazolates, which may have different architectures or supramolecular isomers in the 1:1 metal−ligand ratio (Figure 1).[23] A coordination polymer of Cu^I and 2-methylimidazolate (mim), $[Cu(mim)]_n$, exhibits a

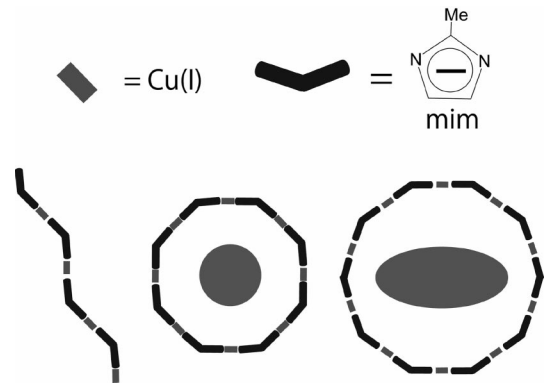

Figure 1. Schematic representation of three structural supramolecular isomers possible for mim and Cu^I: (a) zigzag chain; (b) octagon; (d) decagon.

zigzag chainlike structure. To induce the formation of an open circular structure, the hydrophobic mim methyl groups should point inward in the ring. It can therefore be speculated that, at a certain orientation, a polygonal structure may possibly be formed by templating with hydrophobic, especially circular, organic molecules such as toluene, benzene, and cyclohexane in the reaction system. This speculation led to the isolation of predesigned, organically cornered, uniform molecular octagons $[Cu_8(mim)_8]$ (inner diameter: 0.99 nm), which were generated with the corresponding solvents benzene, toluene, and cyclohexane. Furthermore, higher molecular decagons $[Cu_{10}(mim)_{10}]$ (inner diameter: 1.36 nm) have also been obtained by using larger organic molecules (*p*-xylene and naphthalene) as templates. The use of alkyl-containing bent bridges and hydrophobic circular template molecules should be responsible for the formation of uniform discrete open frameworks.

Flexible ligands with conformational freedom provide significant potential for coordination networks with a large variety of structures and dynamic properties.[24,25] However, by the incorporation of a higher degree of flexibility into the building blocks, the amount of predefined information is reduced, and two or more different structures can arise from identical metal–ligand combinations. 1,2-Bis(4-pyridyl)ethane (bpe) can adopt gauche (angular) or anti (linear) conformations, and $[Co(NO_3)(bpe)_{1.5}]_n$ can exist in at least three different supramolecular isomers, resulting from gauche or anti conformations of the bpe ligand.[26] The reaction of bis(hexafluoroacetylacetonato)manganese(II) trihydrate $[Mn(hfac)_2(H_2O)_3]$, a 90° corner unit, with the flexible linking unit 4,4-trimethylenedipyridine (tmdpy) allows for the potential formation of three different types of solid-state coordination species: infinite helical polymers, closed dimeric systems, and infinite 1D polymers.[27,28] The untemplated starting materials give a coordination helix. The other two possible species can be realized through the selective use of a variety of simple, organic guests: toluene, diphenylmethane, *cis*-stilbene, 1,3-diphenylpropane, benzyl alcohol, nitrobenzene, and cyanobenzene. When solutions of $[Mn(hfac)_2(H_2O)_3]$ and tmdpy are crystallized in the presence of any of these clathrates, the dimeric macrocycles result in all cases, except for that of 1,3-diphenylpropane, in which a syndiotactic, wedge-shaped polymer forms. The crystal packing diagrams for the dimeric macrocycles clearly reveal that the cocrystallized guest molecules act as templates in the formation of the ring system, suppressing any oligomerization that may occur.

A chiral open framework is an important goal because there are many potential applications such as chiral separation and catalysis. Two approaches have been particularly successful in the synthesis of chiral PCPs.[29] The first method uses a chiral organic bridging ligand to link the metal centers in the framework.[30,31] The alternative method uses a chiral template that does not bridge the metal centers but forces bulk chirality. For instance, helical (10,3)-a networks can be generated by binding the achiral tridentate 1,3,5-benzenetricarboxylate (btc) ligand to Ni^{II}.[32,33] The bulk chirality of these intrinsically chiral $[Ni_3(btc)_2]_n$ networks can be controlled by the handedness of a small templating bidentate alcohol molecule (such as propan-1,2-diol) bound to the metal center. The use of a chiral template that does not act as a linker appears to offer considerable scope in the synthesis of chiral frameworks. Recently, a chiral induction effect in ionothermal synthesis was reported.[34] Use of the chiral ionic liquid 1-butyl 3-methylimidazolium L-aspartate produces a homochiral framework from achiral building blocks that crystallizes in the space group $P4_12_12$. Such an effect may open up new opportunities in the preparation of chiral materials.

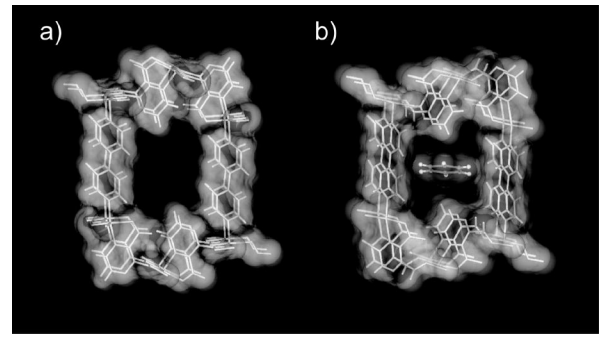

Figure 2. Representation of the pore structures of (a) **CPL-2** and (b) **CPL-2** ⊃ **benzene**. Both views are down from the *a* axis, displayed by stick and van der Waals surface models.

2.2. Secondary TBG: Crystal Structure Transformations Induced by Templates. Recently, there has been growing interest in flexible and dynamic PCPs, in particular, those that reversibly change their structures in response to guest molecules. Previously, we classified the pore behavior of flexible PCPs into four categories:[10] (1) *induced-fit-type pores*,[35–37] (2) *breathing-type pores*,[24,38,39] (3) *guest exchange pores*,[40] and (4) *healing-type pores*.[41] Appropriate guest molecules act as templates and induce these reversible structure transformations. Such host dynamics would be a key principle for molecular sensing and property switching. This dynamic templating effect can be called "secondary TBG".

When induced-fit-type pores accommodate guest molecules, shape-responsive fitting occurs and the guest information strongly affects the host structure. For instance, a PCP with a pillared layer structure (CPL), $[Cu_2(pzdc)_2(bpy)]$ (**CPL-2**; pzdc = pyrazine-2,3-dicarboxylate, bpy = 4,4′-bipyridine), was constructed from stiff motifs of bpy and the pyrazine ring in pzdc, a flexible motif of the carboxyl groups with rotational freedom, and a Cu ion geometry that possesses a degree of flexibility in bond cleavage because of the Jahn–Teller distortion.[37] In situ synchrotron powder X-ray diffraction patterns of **CPL-2** and its benzene-adsorbed form, {$[Cu_2(pzdc)_2(bpy)]$·benzene} (**CPL-2** ⊃ **benzene**), have been measured. The structures of **CPL-2** and **CPL-2** ⊃ **benzene** were determined from Rietveld analysis. The benzene molecules are ordered quite regularly in the 1D channel in a so-called commensurate fashion, and adsorption of benzene in the channels induced a remarkable contraction in the crystal (*b* axis, 6.8%; volume, 4.9%), although the channels were occupied by the benzene molecules (Figure 2). Mutual sliding of the 2D sheets and pore shrinking is observed, which is accompanied by a change in the copper coordination geometry from a square pyramid to a square

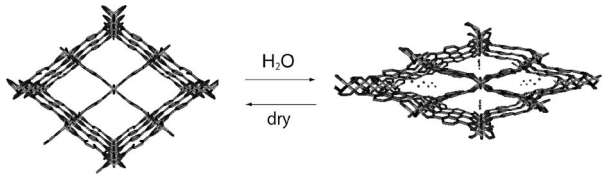

Figure 3. Hydration and dehydration processes occurring in **MIL-53**. Left: **MIL-53HT** (dehydrated). Right: **MIL-53LT** (hydrated).

plane. This crystal transformation provides a pore structure that is well suited to benzene molecules, and we denoted it as a "shape-responsive fitting" transformation. The toluene molecule, on the other hand, is larger and less symmetrical than benzene. From NMR and thermogravimetric analysis, it can be shown that the shape of toluene means it cannot be ordered in commensurate fashion in the channels of **CPL-2** and the population inside the pores is smaller than that with benzene.[42]

The key factors to induce structure transformation are the shape and also the electrical properties such as the dipole or quadrupole moment of the template. A porous carboxylate formed by chains of metallic centers, **MIL-53** [chemical formula M(OH)(bdc) (M = Cr^{3+}, Al^{3+}; bdc = 1,4-benzenedicarboxylate)], exhibits an original shrinking phenomenon upon hydration−dehydration, which involves ca. 5 Å atomic movements (Figure 3).[36,43] The adsorption of carbon dioxide in **MIL-53** is also accompanied by unusual structural phenomena. The dehydrated solid shows a marked two-step adsorption process that has been interpreted as the initial closing of the structure before it reopens at higher pressures.[44,45] This isotherm shape with CO_2 is in contrast to that with other molecules such as CH_4. The adsorption isotherms obtained for CH_4 are typical of those obtained with nanoporous materials such as zeolites and activated carbons. While CO_2 has a significant quadrupole moment (-1.4×10^{-35} C m) that induces crystal structure transformations and specific interactions with adsorbents (such as molecular orientation and hydrogen bonding), CH_4 has no specific moment.

Counteranions in PCPs have roles not only to neutralize the overall charge in the solid but also to regulate frameworks; thus, anion-exchange properties accompany drastic structural conversions.[40,46] Such structure transformation can control the PCP's porous properties. Interpenetrating networks $\{[Ni(bpe)_2(N(CN)_2)]\ (N(CN)_2)(5H_2O)\}_n$ ($N(CN)_2^-$ = dicyanamide) have two types of channels for anionic $N(CN)_2^-$ and neutral water molecules, respectively (Figure 4a).[47] The hydrated framework provides a dual function of specific anion exchange of free $N(CN)_2^-$ for the smaller N_3^- anions and selective gas sorption. The N_3^--exchanged framework leads to a dislocation of the mutual positions of the two interpenetrating frameworks, resulting in an increase in the effective pore size in one of the counterparts of the channels and a higher accommodation of adsorbate than that in the as-synthesized form (Figure 4b). Anion exchange controls the overall framework functionality, resulting in bifunctionality in one compound, thereby paving the way for the fabrication of new materials.

Chirality is of fundamental importance for biological systems as well as in advanced materials such as nonlinear optical devices, enantioselective synthesis, and asymmetric

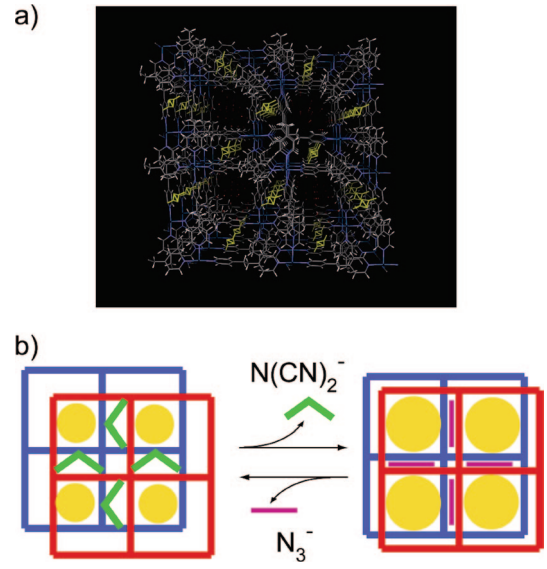

Figure 4. (a) X-ray crystal structure of $\{[Ni(bpe)_2(N(CN)_2)]\text{-}(N(CN)_2)(5H_2O)\}_n$. 3D network of **1** showing two kinds of channels along the crystallographic *c* axis. The rectangular channel accommodates free $N(CN)_2$ anions (yellow), and the hexagonal channel is occupied by water molecules (red). (b) Schematic view of anion exchange, which controls the overall framework functionality.

catalysis and in chiral magnets. It is challenging to design a crystalline material that has chiral−achiral switching properties. The 2D bilayer open framework of Cu^{II}, $\{[Cu(pyrdc)(bpp)](5H_2O)\}_n$ [pyrdc = pyridine-2,3-dicarboxylate; bpp = 1,3-bis(4-pyridyl)propane], shows reversible breathing phenomena with centric-to-acentric structural transformation upon dehydration–rehydration, with retention of single crystallinity.[48] The X-ray crystal structure of $\{[Cu(pyrdc)(bpp)](5H_2O)\}_n$ reveals a 2D bilayer open framework composed of one Cu^{II}, pyrdc, and bpp ligand in the asymmetric unit, and the space group is centric *Pbcn*. Structure determination reveals that, upon dehydration, $\{[Cu(pyrdc)(bpp)]\}_n$ crystallizes in the acentric and polar space group, $Pca2_1$ (orthorhombic). After the dehydrated single crystal is kept in the open atmosphere for 1 week, the cell volume of the crystal increases and the space group changes to the original *Pbcn* (centric). The material is completely converted to the original as-synthesized framework, which accommodates three water molecules per Cu^{II} in the pore, showing reversible centric-to-acentric structural transformation. Acentric structures can be induced by inclusion of achiral guest molecules in the flexible PCPs. The method could be a new approach to obtaining a novel material with controllable optical and/or magnetic activity.[49]

3. TFG: PCP Frameworks Acting as Templates

Nanopores of PCPs have great potential. Molecules in the nanospaces have properties clearly different from those of the corresponding bulk fluids, which is called a space effect. This kind of space effect can be considered as the stabilization effect of micropores, which enables the preparation of an ordered phase of small molecules and/or provides a specific reaction nanoflask. In these cases, the PCP could be considered as TFG. In this section, we present examples of the TFG effect of PCPs.

3.1. Small-Molecule Assemblies in PCPs. Porous properties have attracted the attention of chemists, physicists, and material scientists because of the scientific interest in the formation of molecular assemblies in nanospaces, such as clusters and 1D arrays and in the anomalous physical properties of confined molecules.[50–54] This confinement effect is characteristic of the nanometer-sized spaces of a micropore (pore size <2 nm) because of the restricted pore geometry and the adsorption enhancement effect of multiple attractive interactions exerted from the confronting and neighboring pore walls. PCPs have advantages as templates of cluster formation: (1) well-regulated nanochannels with their crystallinity, (2) designable pore surfaces resulting in various potential pore walls, and (3) a variety of channel shapes ranging from 1D to 3D types. In addition, these features are appropriate for performing direct observation by X-ray crystallography of various molecular assemblies confined in the nanotemplate. Thus, many crystal structure analyses of assembled guest molecules in the nanospaces of PCPs have been reported.

The dynamics and structures of water clusters confined in nanospaces are different from those of bulk water and ice under ambient pressure.[55–57] Studies on confined water are relevant to a number of biological processes, such as hydration of a biological surface, the dynamics of hydrated proteins, and the mobility of water within biological pores. In addition, these processes have become extremely important in the research field of solid proton conductors for fuel cells. A variety of pore surfaces and shapes of PCPs provide original water cluster structures and phase transition phenomena. For instance, within the hydrophobic cage constructed from an electron-deficient aromatic ligand, 2,4,6-tris(4-pyridyl)-1,3,5-triazine, an adamantanoid $(H_2O)_{10}$ cluster is formed and is termed "molecular ice" because this structure is the smallest unit of the naturally occurring I_c-type ice.[58] Neutron diffraction studies show that the oxygen atoms of water molecules interact with the ligand via a $D_2O\cdots\pi$ interaction. This result indicates that the aromatic ligand acts as a Lewis acidic site and dominates the structure of the water cluster. On the other hand, a hydrophilic or hydrogen-bond acceptor surface can play a crucial role in constructing nanoice structures. Trimesic acid (TMA^{3-}) and $[Co^{III}(H_2bim)_3]^{3+}$ (H_2bim = 2,2′-biimidazolate) construct a 1D channel in which hydrogen bonding between the building blocks and the contained water molecules was observed.[59] From X-ray crystal structure analysis at room temperature, the oxygen atoms of the water molecules were highly disordered and diffusion of the water molecules was observed. From differential scanning calorimetry thermograms performed between 262 and 213 K, reversible phase transitions were observed that showed exothermic peaks at 234.5 K during cooling and endothermic peaks at 245 K during heating. This result suggests a phase transition of water in the nanopore. X-ray crystal structure analysis below the normal phase transition temperature revealed that the confined water molecules are recognized as a certain type of "multilayered ice" composed of three-layered nanotube networks, although the porous structure with the 1D channel is retained (Figure 5). The hydrogen-bonded ice nanotube networks are held in the channel by additional hydrogen bonds between the water molecules and the oxygen atoms of TMA^{3-} on the pore surface. The water clustering in a PCP with hydrogen-bonding sites would contribute to a greater understanding of the ice formation mechanism and the properties of water and ice in confined spaces.

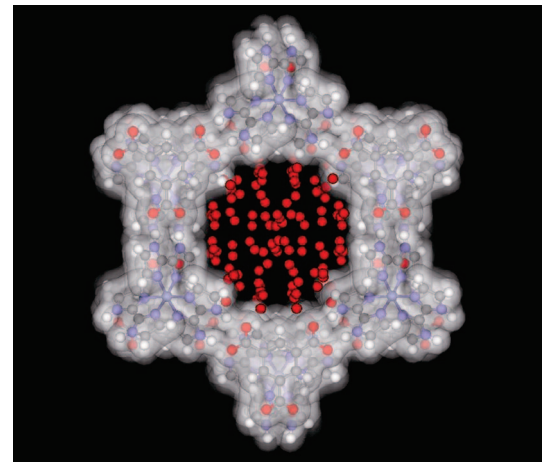

Figure 5. Perspective view along the *c* axis of crystal structures for $[Co^{III}(H_2bim)_3](TMA)$ containing a water cluster below the phase transition temperature of 198 K. The 1D channel in the framework is occupied by water molecules (red).

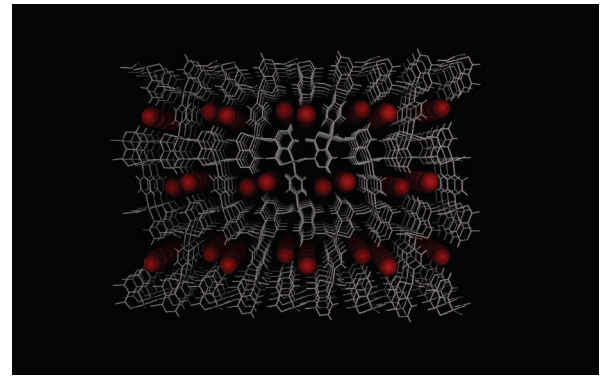

Figure 6. Crystal structure of **CPL-1** with adsorbed O_2 at 90 K. Perspective view down from the *a* axis.

Formation of a low-dimensional assembly of gas molecules is one of the most attractive challenges because of the unusual quantum properties of the simple species.[60] In particular, O_2 is the smallest stable paramagnetic molecule under ambient conditions and has the potential to form new molecular-based magnetic and redox-active materials. A 1D ladder structure of O_2 was formed in a copper coordination polymer, $[Cu_2(pzdc)_2(pyz)]_n$ (**CPL-1**; pyz = pyrazine) with a pore size of 4 × 6 Å^2.[61] The 1D ordered array of O_2 molecules was obtained at 80 kPa (Figure 6). Two O_2 molecules align parallel to each other along the channel direction, and the intermolecular distance is 3.28(4) Å, which is much smaller than the minimum of the Lennard-Jones potential. This intermolecular distance is close to the nearest distance in solid α-O_2, which is stable below 24 K. The magnetic susceptibility for adsorbed O_2 molecules approaches zero with decreasing temperature, indicating a nonmagnetic ground state of the antiferromagnetic dimer $(O_2)_2$. The antiferromagnetic interaction is estimated to be J/k_B = 50 K, which is larger than that of the α phase with J/k_B = 30

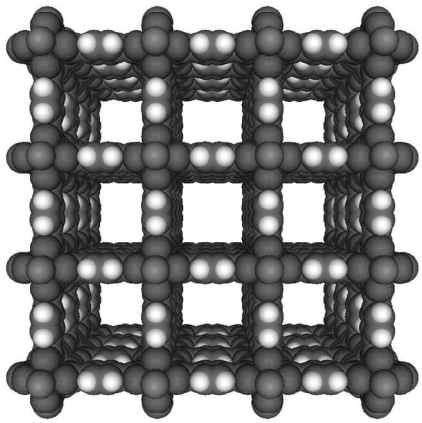

Figure 7. Space-filling representation of $[Zn_2(bdc)_2(ted)]_n$, which emphasizes the open square channels; view along the 4-fold axis.

K. The Raman spectrum of the O_2 stretching vibration mode appears as a sharp peak at a higher energy than that of solid α-O_2 under atmospheric pressure and is comparable to that of α-O_2 under 2 GPa. These results are ascribed to the strong confinement effect of **CPL-1**. In situ synchrotron powder X-ray diffraction measurements revealed that N_2, Ar, and CH_4 also form specific molecular arrays in **CPL-1**, as well as O_2, and the ordered arrays are characteristic of the kind of gas molecule and the geometrical and potential properties of the ultramicropores of **CPL-1**.[62] Such gas arrangements were also observed in flexible PCP frameworks.[63,64] A 1D compound, $[Rh^{II}_2(bza)_4(pyz)]_n$ (bza = benzoate), demonstrates gas adsorption, provided that the interstitial gas molecules are well ordered among the chain motifs.[65] These gas-inclusion crystal structures could be characterized by single-crystal X-ray crystallography. It is interesting that gas molecules are well confined and afford an ordered structure even in the frameworks constructed as 1D coordination chains. These results are useful for the understanding of micropore filling based on the role of micropore geometry and intermolecular interactions, providing information about nanospaces with the potential to discover novel phenomena of molecular assemblies unexplored in the conventional bulk solid and/or gas state.

3.2. Polymerization in PCPs. Crystalline porous compounds can provide specific molecular-level flasks for the reactions of guest molecules. This allows low-dimensional restrained reactions that are different from bulk and solution reactions in conventional flasks. The nanopores of PCPs have a wide range of advantages as reaction spaces, such as regular channel structures, controllable pore size, dynamic and flexible pores, and unique surface potentials and functionality. In particular, polymerization in PCPs would not only allow multilevel control of the polymerization (control of stereoregularity, molecular weight, helicity, and so on) but also provide well-defined nanostructures, permitting fabrication of next-generation materials.[66]

$[M_2(bdc)_2(ted)]_n$ ($M = Zn^{2+}$, Cu^{2+}; ted = triethylenediamine) has regular, continuous, 1D nanochannels with cross sections of 7.5 × 7.5 $Å^2$ (Figure 7).[67,68] The radical polymerization of styrene was performed in these regular, continuous, robust, and relatively wide 1D channels.[69] In this system, polymerization proceeds with high conversion

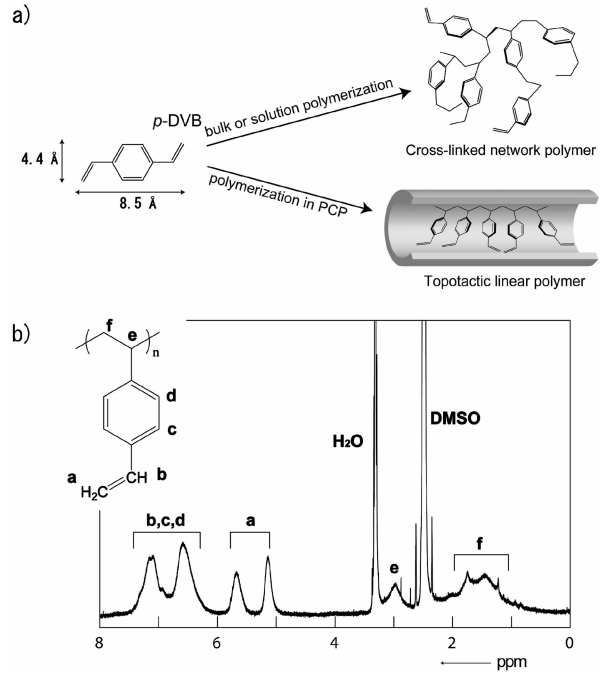

Figure 8. (a) Schematic view of the usual cross-linked network polymerization of *p*-DVBs and topotactic linear polymerization in the 1D channels of PCPs. (b) ^1H NMR spectrum (in DMSO-d_6) of poly(*p*-DVB) obtained from the nanochannels of $[Zn_2(bdc)_2(ted)]_n$. The ratio of the intensities of signal a to those of signals b−d is 2:5.

(71%), without collapse of the channel structures, and the resultant polystyrene is completely encapsulated in the nanochannels. The propagating radical in this system was "living" because of effective protection in the nanochannel. In fact, the number-average molecular weight (M_n) and the polydispersity (M_w/M_n) of the polystyrene recovered from $[M_2(bdc)_2(ted)]_n$ are ≈55 000 and 1.6, respectively. However, the gel permeation chromatography profile of bulk polystyrene synthesized under comparable conditions showed a broad fraction of polymer with a high polydispersity ($M_w/M_n = 4.7$), indicating the possibility of molecular-weight control in the nanochannel of $[M_2(bdc)_2(ted)]_n$. On the other hand, the polymerization of styrene does not proceed efficiently in **CPL-2**, with a pore size comparable to that of $[M_2(bdc)_2(ted)]_n$. Generally, the reactivity of guest molecules in confined nanospaces is strongly dependent on the molecular behaviors. Solid-state ^2H NMR spectra reveal that styrene-$d_8$adsorbed in $[Zn_2(bdc)_2(ted)]_n$ has high mobility and fast rotation in the nanochannels. However, the spectra of styrene-d_8 in **CPL-2** show completely solidlike behavior, even at the polymerization temperature, indicating that the mobility of styrene is much more restricted in **CPL-2** than in $[M_2(bdc)_2(ted)]_n$. This restricted arrangement of the styrene in the nanochannel of **CPL-2** resulted in poor reactivity. The pore size and shape are key factors in promoting polymerization in PCPs.

In radical polymerization processes, control of the polymer primary structures, which is essential for the fabrication of desired regularities and topologies, is incredibly difficult because of the high reactivity of the growing radical species. In particular, controlled radical polymerization of divinylbenzenes (DVBs) to attain a regulated low-dimensional chain growth is still undeveloped because both vinyl moieties in

these DVBs are equally reactive and therefore radical polymerization results in the formation of a hyperbranched network polymer. Recently, a selective linear radical polymerization of DVBs was demonstrated in the channels of $[Zn_2(bdc)_2(ted)]_n$ (Figure 8).[70] In the ^{1}H NMR spectrum of the resultant poly(*p*-DVB), signals can be assigned to protons at the β-carbon of the vinyl groups (δ 5.1 and 5.7 ppm) (Figure 8b). A comparison of the integrated peak intensities of the aromatic and vinyl regions shows that only one vinyl group of *p*-DVB is selectively polymerized to form the linear polymer and that hardly any undesired kink structures (branching and/or bonding through both vinyl groups) are formed during the reaction. The prerequisite for the topotactic selective radical polymerization is a template nanospace that has an appropriate channel size and shape to allow monomer adsorption and arrangement.

Much attention has been directed to the electronic and optical properties of poly(substituted acetylenes) for a wide range of applications such as conducting materials, nonlinear optics, polymer sensors, and components in molecular electronics.[71] In particular, the design and understanding of well-defined nanostructures based on such π-conjugated polymers is one of the most challenging goals in contemporary polymer and solid-state sciences for their future application in the creation of nanosized molecule-based devices.[72–74] Controlled and selective polymerizations of substituted acetylenes were demonstrated in 1D specific nanochannels of **CPL-2** with basic carboxylate oxygen atoms as catalytic interaction sites on the pore walls.[75] With acidic monosubstituted acetylenes, the basic oxygen atoms from the carboxylate ligands in **CPL-2** produce reactive acetylide species that subsequently initiate anionic polymerization in the nanochannel. This unique catalytic polymerization mechanism in **CPL-2** is supported by IR spectroscopy measurements and computer simulation with a universal force field. Such precisely aligned PCP nanochannels filled with π-conjugated substituted polyacetylenes should be a promising new class of host–guest nanostructures for applications such as nanoscale electronics and for fundamental investigations of these polymers in the isolated, single-chain state.

4. Templates for Function Design

Much effort has been devoted to the design of functional molecular assemblies toward their potential applications such as magnetism, electrical conductivity, dielectric properties, molecule or ion storage, and heterogeneous catalysis, using TBG voids in PCP frameworks resulting from the removal of guests. This synthetic process controls the pore size and shape and is therefore regarded as one way by which the structural properties of template molecules are transcribed into the pore structure. On the other hand, the TFG process causes guest molecules or ions to form assemblies in porous frameworks, resulting in new types of nanohybrid structures. This is also a role of the framework. Interestingly, coordination polymers are so uniquely flexible that the framework and/or electronic properties may respond to external chemical and physical stimuli. On this basis, we could expect the symbiotic cooperation of both frameworks and guests for both the structures and their functions.

Flexible frameworks provide pore structures that are suitable for given guest molecules and much more useful for molecular recognition or selective guest inclusion than are robust porous structures. Coupling of structure flexibility and adsorption properties is a key principle for selective adsorption. Furthermore, of considerable interest is the interplay of hosts and guests for chemical and/or physical properties, resulting in synergy effects and cooperative properties. Such strong coupling between host and guest can be achieved by electron donor–acceptor interaction or correlation in either ground or excited states, and, therefore, the precise arrangement of redox-active π systems and active metal sites is of significance. In this section, we present a strategy aimed at not only structure but also function, utilizing the template effect in PCPs.

4.1. Size- and Shape-Fixing Templates in Space Structure Flexible PCPs. Channel surface modification of PCPs is essential for the creation of functionalized porous structures.[76] When the multiple specific interaction sites, such as open metal sites or metal and free organic groups, are located at suitable positions on the regular micropore, an adsorption system specific to the target molecule can be realized.[77] In addition, several PCPs have flexible or dynamic natures. The state of the host component without guest molecules is referred to as the "apohost". Guest-selective structure transformation would lead to highly selective porous materials. The TBG pathway can be used to synthesize PCPs with selective adsorption properties. Not only can the primary TBG effect play an integral role in the solid-state assembly process itself, but it can also determine the chemical properties of the pore surface. When PCPs are synthesized with template molecules, the templates act as placeholders and the structure of the template is transcribed into the pore shape. When we step further, we could design systems in which template molecules are located at the appropriate positions in the pores for a specific interaction between guests and the pore surface. Furthermore, when the well-designed PCP has a flexible nature, structure transformations from the closed phase to the open phase are induced by appropriate template molecules. Such secondary TBG effects can be a key principle for selective adsorption properties.

A PCP, $\{[Cu^{I}_3(CN)_3(hat(CN)_3(OEt)_3]\cdot 3THF\}_n$ (hat = hexaazatriphenylene), was prepared in a EtOH/THF solution.[78,79] There are two kinds of pores in this structure: one is a large 1D channel running along the *c* axis with a cross section of 10×10 Å^2, and the other pore is just a cavity located along the channel in which the hat units form a floor and a ceiling and their portals open to three adjacent channels. A THF molecule is included in the cavity as a template molecule (Figure 9a). The oxygen atom of THF interacts with the π plane of hat, thus defining an interaction between an electron-deficient aromatic ring and an electronegative atom. Furthermore, removal of the THF molecules from the PCP results in a decrease in the regularity over a wide range, leading to low porosity. This apohost is reconstructed to its regular porous form by guests having electronegative atoms, in particular, pyrazine (pyz) and 1,4-dioxan (dox), which have sizes suitable for the cavity. In contrast, the PCP does not adsorb hydrocarbons, linear ethers

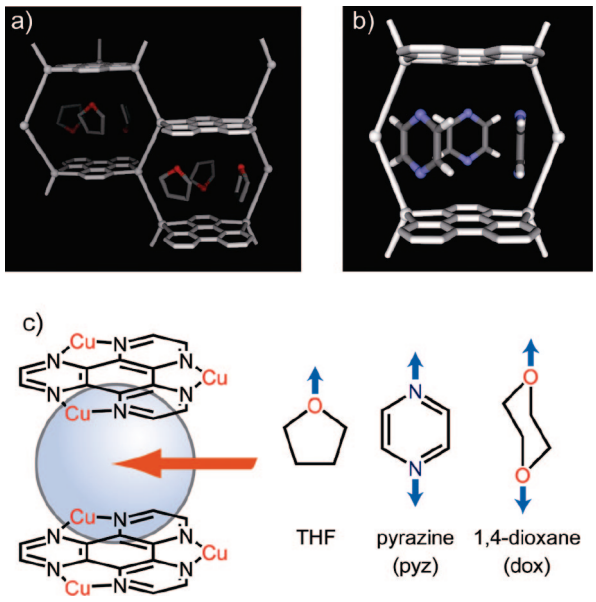

Figure 9. (a) Crystal structure of the cavity defined by two hat molecules containing template THF (O, red; C, gray). (b) Crystal structure of the cavity containing pyz (N, blue; C, gray). (c) Schematic view of the inclusion of guest molecules into pores comprising π planes.

and alcohols, or large molecules. The results of crystallographic analysis and solid-state ^{2}H NMR spectra of the pyz-adsorbed form reveal that the pyz molecules behave as if the two nitrogen atoms at both ends of the molecule bind with the two π planes of hat moieties, resembling a pillar (Figure 9b). The multiple interactions and reversible host framework flexibility would influence the guest-selective structure transformation and adsorption property of the PCPs (Figure 9c).

A PCP of $\{[Zn(\mu_4\text{-TCNQ}-\text{TCNQ})bpy]\cdot 1.5benzene\}_n$ was synthesized by reacting $Zn(NO_3)_2\cdot 6H_2O$ with LiTCNQ (TCNQ = 7,7,8,8-tetracyano-*p*-quinodimethane) and bpy in a MeOH/benzene mixture (1:1).[80] $[TCNQ-TCNQ]^{2-}$ acts as a cross-linker connecting the four Zn−bpy chains of Zn ions and bpy to form a 3D open framework. The channels delimited by the ligands are of the undulating form, not straight but a unique form comprising an alternating arrangement of two types of tubes of large and small diameters. The large-diameter space is adequate to accommodate a benzene molecule because of the suitability of the cavity's size and thickness. When benzene was not added to the reaction mixture and the other conditions were kept unchanged, the reaction produced a different PCP, indicating that benzene acts as a template.[81] The guest benzene molecule is accommodated strongly in the cavity with the size effect and the CH−π interaction with the host framework. In the benzene removal process, the crystal is transformed to a guest-free crystal phase, $\{[Zn(\mu_4\text{-TCNQ}-\text{TCNQ})bpy]\}_n$. The sorption isotherms of benzene and cyclohexane at 298 K were measured, and the profiles obviously differed. With benzene, no adsorption occurred in the lower relative pressure region, although an abrupt increase in adsorption and a decrease in the relative pressure were observed in the higher pressure region. This is similar to the gate-open-type adsorption behavior that is related to the structural transformation of the host framework. The driving force to open the gates could be the presence of a higher-affinity interaction of the pore surface and guest molecules. In contrast, no adsorption of cyclohexane occurs even in the higher relative pressure region, indicating that the gates remain closed for cyclohexane. The keys to the success of the selective adsorption property are the H-π-type host–guest interaction, which triggers the structural transformation from the closed form to the open form in the sorption process and the undulating channel with cages fitting tightly to the shape of benzene.

4.2. Donor–Acceptor-Inducing Templates in Flexible PCPs: Electronic Structure Flexibility. Charge-transfer (CT) or electron-transfer (ET) interactions between PCPs and guest molecules can affect both host and guest electronic properties. Such CT and ET interactions are sometimes strong enough to cause reactions between the PCP and the guests. For example, when a PCP with a redox-active nickel macrocycle was immersed in solutions of Ag^+ and Au^+ at room temperature, solids including silver and gold nanoparticles, respectively, were formed by the redox reaction with the nickel ions incorporated in the PCP.[82–84] In addition, nanoscale organization of electron donor–acceptor π-conjugated systems plays a crucial role in facilitating energy-transfer, CT, and ET processes in natural and artificial-light energy conversion systems.[74,85–87] One of the most effective and attractive approaches for the assembly of such π systems is the use of PCPs, composed of redox-active π systems. This is because PCPs with π-electron systems can serve as templates for the incorporation of redox-active and/or photoactive molecules into their nanosized spaces. Template effects of PCPs containing π systems could lead to potentially useful new classes of host–guest nanostructures.

TCNQ is a well-known multi-redox-active ligand that can act as a good acceptor and a weak or a strong donor when its valence is 0, −1, or −2, respectively. The CT interaction between the host framework and a guest molecule would occur if TCNQ were directly incorporated into the pore walls of a polymer. We obtained a redox-active 3D coordination framework $[Zn(TCNQ)bpy]_n$, synthesized by the reaction of $TCNQ^-$, Zn ions, and bpy, which demonstrates a unique guest accommodation accompanying the CT interaction.[81] The charge valence of TCNQ in the crystal is estimated to be −2 (Zn, 2+; TCNQ, 2−; bpy, 0) because no counteranion is observed in the cavity. The mechanism for the formation of the $TCNQ^{2-}$ dianion is not clear, but it may arise as a consequence of a disproportionation reaction of $TCNQ^-$. The UV–vis spectra of $[Zn(TCNQ)bpy]_n$ with aromatic molecules as guests reveal that significant color changes occurred, which are associated with the electron-accepting characteristics of the guest molecule. This is ascribed to the CT interaction between TCNQ and the aromatic molecule.

A PCP containing an anthracene derivative, $\{[Zn_2(adc)_2(ted)]\}_n$ (adc = 9,10-anthracenedicarboxylate), has been synthesized.[88] Single-crystal X-ray analysis demonstrated that the 3D porous network is based on 2D layers of $\{[Zn(adc)]\}_n$, constructed from paddle-wheel units and pillars of ted, affording 2D channels (Figure 10a). An adsorbed guest molecule is expected to interact with the accessible anthracene π planes. An emission spectrum curve of

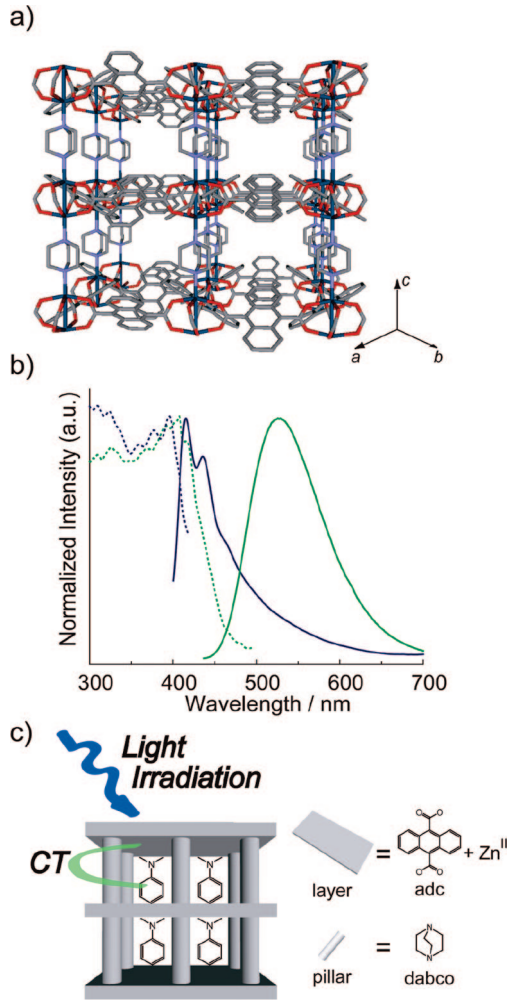

Figure 10. (a) Crystal structures of $\{[Zn_2(adc)_2(ted)]\}_n$ drawn from the [110] direction. The gray, purple, red, and dark-blue colors represent carbon, nitrogen, oxygen, and zinc, respectively. (b) Excitation (dashed line) and emission (solid line) spectra of $\{[Zn_2(adc)_2(ted)]\}_n$ (blue) and $\{[Zn_2(adc)_2(ted)]\cdot DMA\}_n$ (green). The excitation wavelengths are 376 and 410 nm, respectively. (c) Schematic illustration of a host–guest nanocomposite.

$\{[Zn_2(adc)_2(ted)]\}_n$ displays an emission maximum at 415 nm, with a vibrational band at 436 nm. The spectrum can be assigned to an emission from the monomeric anthracene. On the other hand, the emission spectrum of the *N*,*N*-dimethylaniline (DMA)-adsorbed form, $\{[Zn_2(adc)_2(ted)]\cdot DMA\}_n$, is quite different from that of $\{[Zn_2(adc)_2(ted)]\}_n$. Complete quenching occurs in the excited-state fluorescence of monomeric anthracene, and a new broad emission band appears from 400 to 700 nm (Figure 10b). The emission with a large Stokes shift represents a photoinduced CT complex between the host anthracene unit (electron acceptor) and the guest DMA molecules (electron donor). In general, such a CT emission is inefficient because its transition dipole moment is lower than that of fluorescence, that is, for the transition from the singlet excited state to the ground state of the individual components. The complete quenching of monomeric anthracene emission and the highly efficient emission of the DMA-adsorbed form originate from the confined configuration of DMA in the nanopores. In addition, the electron-donor guests and electron-acceptor 2D sheets define an alternating layered structure (Figure 10c). Because of its regularity and the close contact in the micropore, an efficient interaction can be obtained. Such hybrid materials composed of individual arrays of electron-donor and -acceptor molecules are promising advances toward the efficient conversion of light energy into electrical energy.[89,90] Precisely aligned PCP nanochannels filled with guest molecules should be a promising new class of nanostructures with host–guest synergy effects for applications such as nanoscale electronics. The template effect of PCPs with redox-active modules could provide a molecular design strategy to achieve novel host–guest nano-ordered materials.

5. Conclusion

This review has summarized templating effects in PCPs and has shown why this subject is so attractive for new porous materials. Much effort has been devoted to the design of nano-ordered molecular-based materials. The template effects defined as TFG and TBG in PCP controls the nanoscale voids and molecular assemblies, respectively. The symbiotic combination of TFG and TBG is a conceptual approach to this subject, and novel porous properties could be realized first in flexible PCPs.

References

(1) Yaghi, O. M.; O'Keeffe, M.; Ockwig, N. W.; Chae, H. K.; Eddaoudi, M.; Kim, J. *Nature* **2003**, *423* (6941), 705–714.
(2) Rosseinsky, M. J. *Microporous Mesoporous Mater.* **2004**, *73* (1–2), 15–30.
(3) Férey, G.; Mellot-Draznieks, C.; Serre, C.; Millange, F. *Acc. Chem. Res.* **2005**, *38* (4), 217–225.
(4) Maspoch, D.; Ruiz-Molina, D.; Veciana, J. *J. Mater. Chem.* **2004**, *14* (18), 2713–2723.
(5) Mueller, U.; Schubert, M.; Teich, F.; Puetter, H.; Schierle-Arndt, K.; Pastre, J. *J. Mater. Chem.* **2006**, *16* (7), 626–636.
(6) Collins, D. J.; Zhou, H. C. *J. Mater. Chem.* **2007**, *17* (30), 3154–3160.
(7) Kitagawa, S.; Kitaura, R.; Noro, S. *Angew. Chem., Int. Ed.* **2004**, *43* (18), 2334–2375.
(8) Fletcher, A. J.; Thomas, K. M.; Rosseinsky, M. J. *J. Solid State Chem.* **2005**, *178* (8), 2491–2510.
(9) Kitagawa, S.; Uemura, K. *Chem. Soc. Rev.* **2005**, *34* (2), 109–119.
(10) Uemura, K.; Matsuda, R.; Kitagawa, S. *J. Solid State Chem.* **2005**, *178* (8), 2420–2429.
(11) Kresge, C. T.; Leonowicz, M. E.; Roth, W. J.; Vartuli, J. C.; Beck, J. S. *Nature* **1992**, *359* (6397), 710–712.
(12) Kaneko, K.; Murata, K. *Adsorption* **1997**, *3* (3), 197–208.
(13) Langley, P. J.; Hulliger, J. *Chem. Soc. Rev.* **1999**, *28* (5), 279–291.
(14) Schuth, F. *Angew. Chem., Int. Ed.* **2003**, *42* (31), 3604–3622.
(15) Blake, A. J.; Champness, N. R.; Hubberstey, P.; Li, W. S.; Withersby, M. A.; Schröder, M. *Coord. Chem. Rev.* **1999**, *183*, 117–138.
(16) Moulton, B.; Zaworotko, M. J. *Chem. Rev.* **2001**, *101* (6), 1629–1658.
(17) Hosseini, M. W. *Acc. Chem. Res.* **2005**, *38* (4), 313–323.
(18) Eddaoudi, M.; Moler, D. B.; Li, H. L.; Chen, B. L.; Reineke, T. M.; O'Keeffe, M.; Yaghi, O. M. *Acc. Chem. Res.* **2001**, *34* (4), 319–330.
(19) Masaoka, S.; Tanaka, D.; Nakanishi, Y.; Kitagawa, S. *Angew. Chem., Int. Ed.* **2004**, *43* (19), 2530–2534.
(20) Batten, S. R.; Robson, R. *Angew. Chem., Int. Ed.* **1998**, *37* (11), 1460–1494.
(21) Biradha, K.; Domasevitch, K. V.; Moulton, B.; Seward, C.; Zaworotko, M. J. *Chem. Commun.* **1999**, (14), 1327–1328.
(22) Biradha, K.; Fujita, M. *Dalton Trans.* **2000**, (21), 3805–3810.
(23) Huang, X. C.; Zhang, J. P.; Chen, X. M. *J. Am. Chem. Soc.* **2004**, *126* (41), 13218–13219.
(24) Kitaura, R.; Fujimoto, K.; Noro, S.; Kondo, M.; Kitagawa, S. *Angew. Chem., Int. Ed.* **2002**, *41* (1), 133–135.
(25) Kasai, K.; Fujita, M. *Chem.—Eur. J.* **2007**, *13* (11), 3089–3105.
(26) Hennigar, T. L.; MacQuarrie, D. C.; Losier, P.; Rogers, R. D.; Zaworotko, M. J. *Angew. Chem., Int. Ed.* **1997**, *36* (9), 972–973.
(27) Tabellion, F. M.; Seidel, S. R.; Arif, A. M.; Stang, P. J. *Angew. Chem., Int. Ed.* **2001**, *40* (8), 1529.
(28) Tabellion, F. M.; Seidel, S. R.; Arif, A. M.; Stang, P. J. *J. Am. Chem. Soc.* **2001**, *123* (48), 11982–11990.
(29) Kesanli, B.; Lin, W. B. *Coord. Chem. Rev.* **2003**, *246* (1–2), 305–326.
(30) Seo, J. S.; Whang, D.; Lee, H.; Jun, S. I.; Oh, J.; Jeon, Y. J.; Kim, K. *Nature* **2000**, *404* (6781), 982–986.
(31) Wu, C. D.; Hu, A.; Zhang, L.; Lin, W. B. *J. Am. Chem. Soc.* **2005**, *127* (25), 8940–8941.

(32) Kepert, C. J.; Prior, T. J.; Rosseinsky, M. J. *J. Am. Chem. Soc.* **2000**, *122* (21), 5158–5168.
(33) Bradshaw, D.; Prior, T. J.; Cussen, E. J.; Claridge, J. B.; Rosseinsky, M. J. *J. Am. Chem. Soc.* **2004**, *126* (19), 6106–6114.
(34) Lin, Z. J.; Slawin, A. M. Z.; Morris, R. E. *J. Am. Chem. Soc.* **2007**, *129* (16), 4880.
(35) Millange, F.; Serre, C.; Férey, G. *Chem. Commun.* **2002**, (8), 822–823.
(36) Serre, C.; Millange, F.; Thouvenot, C.; Nogues, M.; Marsolier, G.; Louer, D.; Férey, G. *J. Am. Chem. Soc.* **2002**, *124* (45), 13519–13526.
(37) Matsuda, R.; Kitaura, R.; Kitagawa, S.; Kubota, Y.; Kobayashi, T. C.; Horike, S.; Takata, M. *J. Am. Chem. Soc.* **2004**, *126* (43), 14063–14070.
(38) Maji, T. K.; Uemura, K.; Chang, H. C.; Matsuda, R.; Kitagawa, S. *Angew. Chem., Int. Ed.* **2004**, *43* (25), 3269–3272.
(39) Kitaura, R.; Seki, K.; Akiyama, G.; Kitagawa, S. *Angew. Chem., Int. Ed.* **2003**, *42* (4), 428.
(40) Noro, S.; Kitaura, R.; Kondo, M.; Kitagawa, S.; Ishii, T.; Matsuzaka, H.; Yamashita, M. *J. Am. Chem. Soc.* **2002**, *124* (11), 2568–2583.
(41) Uemura, K.; Kitagawa, S.; Fukui, K.; Saito, K. *J. Am. Chem. Soc.* **2004**, *126* (12), 3817–3828.
(42) Horike, S.; Matsuda, R.; Kitagawa, S. *Stud. Surf. Sci. Catal.* **2005**, *156*, 725–732.
(43) Loiseau, T.; Serre, C.; Huguenard, C.; Fink, G.; Taulelle, F.; Henry, M.; Bataille, T.; Férey, G. *Chem.—Eur. J.* **2004**, *10* (6), 1373–1382.
(44) Bourrelly, S.; Llewellyn, P. L.; Serre, C.; Millange, F.; Loiseau, T.; Férey, G. *J. Am. Chem. Soc.* **2005**, *127* (39), 13519–13521.
(45) Llewellyn, P. L.; Bourrelly, S.; Serre, C.; Filinchuk, Y.; Férey, G. *Angew. Chem., Int. Ed.* **2006**, *45* (46), 7751–7754.
(46) Gimeno, N.; Vilar, R. *Coord. Chem. Rev.* **2006**, *250* (23–24), 3161–3189.
(47) Maji, T. K.; Matsuda, R.; Kitagawa, S. *Nat. Mater.* **2007**, *6* (2), 142–148.
(48) Maji, T. K.; Mostafa, G.; Matsuda, R.; Kitagawa, S. *J. Am. Chem. Soc.* **2005**, *127* (49), 17152–17153.
(49) Zhang, B.; Wang, Z. M.; Kurmoo, M.; Gao, S.; Inoue, K.; Kobayashi, H. *Adv. Funct. Mater.* **2007**, *17* (4), 577–584.
(50) Morishige, K.; Kawano, K. *J. Phys. Chem. B* **2000**, *104* (13), 2894–2900.
(51) Kanda, H.; Miyahara, M.; Higashitani, K. *Langmuir* **2000**, *16* (22), 8529–8535.
(52) Holman, K. T.; Pivovar, A. M.; Ward, M. D. *Science* **2001**, *294* (5548), 1907–1911.
(53) Atwood, J. L.; Barbour, L. J.; Jerga, A. *Science* **2002**, *296* (5577), 2367–2369.
(54) Hertzsch, T.; Budde, F.; Weber, E.; Hulliger, J. *Angew. Chem., Int. Ed.* **2002**, *41* (13), 2281–2284.
(55) Ludwig, R. *Angew. Chem., Int. Ed.* **2001**, *40* (10), 1808–1827.
(56) Ohba, T.; Kanoh, H.; Kaneko, K. *J. Am. Chem. Soc.* **2004**, *126* (5), 1560–1562.
(57) Morishige, K.; Yasunaga, H.; Denoyel, R.; Wernert, V. *J. Phys. Chem. C* **2007**, *111* (26), 9488–9495.
(58) Yoshizawa, M.; Kusukawa, T.; Kawano, M.; Ohhara, T.; Tanaka, I.; Kurihara, K.; Niimura, N.; Fujita, M. *J. Am. Chem. Soc.* **2005**, *127* (9), 2798–2799.
(59) Tadokoro, M.; Fukui, S.; Kitajima, T.; Nagao, Y.; Ishimaru, S.; Kitagawa, H.; Isobe, K.; Nakasuji, K. *Chem. Commun.* **2006**, (12), 1274–1276.
(60) Kitagawa, S. *Nature* **2006**, *441* (7093), 584–585.
(61) Kitaura, R.; Kitagawa, S.; Kubota, Y.; Kobayashi, T. C.; Kindo, K.; Mita, Y.; Matsuo, A.; Kobayashi, M.; Chang, H. C.; Ozawa, T. C.; Suzuki, M.; Sakata, M.; Takata, M. *Science* **2002**, *298* (5602), 2358–2361.
(62) Kitaura, R.; Matsuda, R.; Kubota, Y.; Kitagawa, S.; Takata, M.; Kobayashi, T. C.; Suzuki, M. *J. Phys. Chem. B* **2005**, *109* (49), 23378–23385.
(63) Takamizawa, S.; Nakata, E.; Akatsuka, T. *Angew. Chem., Int. Ed.* **2006**, *45* (14), 2216–2221.
(64) Kobayashi, T. C.; Matsuo, A.; Suzuki, M.; Kindo, K.; Kitaura, R.; Matsuda, R.; Kitagawa, S. *Prog. Theor. Phys. Suppl.* **2005**, (159), 271–279.
(65) Kachi-Terajima, C.; Akatsuka, T.; Kohbara, M.; Takamizawa, S. *Chem.—Asian J.* **2007**, *2* (1), 40–50.
(66) Uemura, T.; Horike, S.; Kitagawa, S. *Chem.—Asian J.* **2006**, *1* (1–2), 36–44.
(67) Seki, K.; Takamizawa, S.; Mori, W. *Chem. Lett.* **2001**, (4), 332–333.
(68) Dybtsev, D. N.; Chun, H.; Kim, K. *Angew. Chem., Int. Ed.* **2004**, *43* (38), 5033–5036.
(69) Uemura, T.; Kitagawa, K.; Horike, S.; Kawamura, T.; Kitagawa, S.; Mizuno, M.; Endo, K. *Chem. Commun.* **2005**, (48), 5968–5970.
(70) Uemura, T.; Hiramatsu, D.; Kubota, Y.; Takata, M.; Kitagawa, S. *Angew. Chem., Int. Ed.* **2007**, *46* (26), 4987–4990.
(71) Lam, J. W. Y.; Tang, B. Z. *Acc. Chem. Res.* **2005**, *38* (9), 745–754.
(72) Cardin, D. J. *Adv. Mater.* **2002**, *14* (8), 553–563.
(73) Sozzani, P.; Comotti, A.; Bracco, S.; Simonutti, R. *Angew. Chem., Int. Ed.* **2004**, *43* (21), 2792–2797.
(74) Hoeben, F. J. M.; Jonkheijm, P.; Meijer, E. W.; Schenning, A. P. H. J. *Chem. Rev.* **2005**, *105* (4), 1491–1546.
(75) Uemura, T.; Kitaura, R.; Ohta, Y.; Nagaoka, M.; Kitagawa, S. *Angew. Chem., Int. Ed.* **2006**, *45* (25), 4112–4116.
(76) Higuchi, M.; Horike, S.; Kitagawa, S. *Supramol. Chem.* **2007**, *19* (1–2), 75–78.
(77) Matsuda, R.; Kitaura, R.; Kitagawa, S.; Kubota, Y.; Belosludov, R. V.; Kobayashi, T. C.; Sakamoto, H.; Chiba, T.; Takata, M.; Kawazoe, Y.; Mita, Y. *Nature* **2005**, *436* (7048), 238–241.
(78) Tanaka, D.; Masaoka, S.; Horike, S.; Furukawa, S.; Mizuno, M.; Endo, K.; Kitagawa, S. *Angew. Chem., Int. Ed.* **2006**, *45* (28), 4628–4631.
(79) Masaoka, S.; Tanaka, D.; Kitahata, H.; Araki, S.; Matsuda, R.; Yoshikawa, K.; Kato, K.; Takata, M.; Kitagawa, S. *J. Am. Chem. Soc.* **2006**, *128* (49), 15799–15808.
(80) Shimomura, S.; Horike, S.; Matsuda, R.; Kitagawa, S. *J. Am. Chem. Soc.* **2007**, *129* (36), 10990.
(81) Shimomura, S.; Matsuda, R.; Tsujino, T.; Kawamura, T.; Kitagawa, S. *J. Am. Chem. Soc.* **2006**, *128* (51), 16416–16417.
(82) Suh, M. P.; Moon, H. R.; Lee, E. Y.; Jang, S. Y. *J. Am. Chem. Soc.* **2006**, *128* (14), 4710–4718.
(83) Moon, H. R.; Kim, J. H.; Suh, M. P. *Angew. Chem., Int. Ed.* **2005**, *44* (8), 1261–1265.
(84) Choi, H. J.; Suh, M. P. *J. Am. Chem. Soc.* **2004**, *126* (48), 15844–15851.
(85) Grimsdale, A. C.; Mullen, K. *Angew. Chem., Int. Ed.* **2005**, *44* (35), 5592–5629.
(86) Van der Auweraer, M.; De Schryver, F. C. *Nat. Mater.* **2004**, *3* (8), 507–508.
(87) Schenning, A. P. H. J.; Meijer, E. W. *Chem. Commun.* **2005**, (26), 3245–3258.
(88) Tanaka, D.; Horike, S.; Kitagawa, S.; Ohba, M.; Hasegawa, M.; Ozawa, Y.; Toriumi, K. *Chem. Commun.* **2007**, (30), 3142–3144.
(89) Kang, S. C.; Umeyama, T.; Ueda, M.; Matano, Y.; Hotta, H.; Yoshida, K.; Isoda, S.; Shiro, M.; Imahori, H. *Adv. Mater.* **2006**, *18* (19), 2549.
(90) Yamamoto, Y.; Fukushima, T.; Suna, Y.; Ishii, N.; Saeki, A.; Seki, S.; Tagawa, S.; Taniguchi, M.; Kawai, T.; Aida, T. *Science* **2006**, *314* (5806), 1761–1764.

CM7031866